J Sol-Gel Sci Technol (2008) 46:195–200
DOI 10.1007/s10971-008-1677-4

ORIGINAL PAPER

Sol–gel immobilization of SiO_2/TiO_2 on hydrophobic clay and its removal of methyl orange from water

Xiangfu Meng · Zhongzhong Qian · Haitao Wang · Xiaowei Gao · Shimin Zhang · Mingshu Yang

Received: 28 October 2007 / Accepted: 2 January 2008 / Published online: 6 February 2008

Abstract In this study, SiO_2/TiO_2–organoclay hybrids with high adsorption capability and high photocatalytic activity were synthesized by immobilizing mixed silica and titanium dioxide nanoparticles on organically modified clay via a hydrothermal sol–gel method. Addition of negatively charged silica particles enhanced the uniform dispersion of titanium dioxide nanoparticles on organoclay layers by decreasing the system tension, which resulted in high photocatalytic activity of SiO_2/TiO_2–organoclay hybrids. The high adsorption capability endowed by organically modified clay enriched the organic compounds around the photoactive sites, and thus greatly improved the photodegradation efficiency. Combining the high adsorption capability of organoclay with the high photocatalytic activity of TiO_2 nanoparticles, SiO_2/TiO_2–organoclay hybrids were promising and cost-effective photocatalysts in removal of pollutants from wastewater.

Keywords Adsorption · Organoclay · Photocatalyst · Sol–gel · Titanium dioxide

1 Introduction

The increasing effluent of industrial wastewater has brought many serious environmental problems. Organic compounds in wastewater have adverse impacts on human health, particularly as these compounds are often mutagenic or carcinogenic in nature. Traditional treatment methods through directly physical removal cannot fundamentally eliminate the pollutants, and often cause secondary pollution of environment. Accordingly, it has led to an expanding demand for efficient and economical water treatment procedures.

Organically modified clay can effectively adsorb the organic compounds in wastewater because of its unique layered structure, large surface area and ion-exchange capability [1–3]. Replacement of exchangeable inorganic cations (Na^+ or Ca^{2+}) in the interlayer with quaternary ammonium cations, $[(CH_3)_3NR]^+$ or $[(CH_3)_2NR_2]^+$, where R is a large alkyl hydrocarbon, can greatly improve the adsorption capability for organic contaminants [4–7]. In the past several decades, extensive studies have proved that clay mineral with organic modification could be used as a promising class of adsorbent materials for removing organic contaminants in water. For example, Dentel et al. [8] enhanced the adsorption capability of homoionic Na^+ or Ca^{2+} based montmorillonite for phenol, trichlorophenol and tannic acid by surfactant treatment with dimethyldistearylammonium chloride. Koh et al. [9] prepared organo-minerals from Na-montmorillonite, sericite and zeolite by exchanging quaternary ammonium cations with various carbon chain lengths. They found the uptake capability of aromatic hydrocarbons by organo-minerals was related to the cation exchange capacity and their interlayer expansion. After adsorption, organic molecules were bound within the space enclosed by the silicate lamellae. In addition, the advantage of hydrophobic organoclay was that it was easy to separate from purified water. Therefore, organoclay is an effective and economic adsorbent for removal of contaminants from wastewater.

Nanoscale titanium dioxide has been utilized to photodecompose various organic compounds in air or water due to its high photoactivity, non-toxicity, chemical stability,

X. Meng · Z. Qian · H. Wang · X. Gao · S. Zhang · M. Yang (✉)
Beijing National Laboratory for Molecular Science, Key Laboratory of Engineering Plastics, Institute of Chemistry, Chinese Academy of Sciences, Beijing 100080, China
e-mail: yms@iccas.ac.cn

and low cost [10–13]. However, it is difficult to recover ultrafine TiO_2 particles from suspensions after purification procedure. Immobilization of TiO_2 nanoparticles on substrates is an effective method to resolve the problem. For instance, Ao et al. [14] reported an improved photocatalyst TiO_2 supported on glass fiber filter for indoor air purification. The high surface area of TiO_2 immobilized on glass fiber filter led to a higher activity than commercial photocatalyst, P25. Xu et al. [15] supported TiO_2 photocatalyst on microporous and mesoporous zeolites using sol–gel method. The porous structure in zeolite prevented the growth of large TiO_2 crystallites and prevented conversion to rutile phase in heat treatment. Recently, supporting TiO_2 nanoparticles on clay minerals has attracted extensive attention. Bhattacharyya et al. [16] impregnated TiO_2 on pillared structure montmorillonite and found that the overall removal efficiency of orange II was better than that of bare TiO_2. Kun et al. [17] prepared TiO_2/montmorillonite composites via heterocoagulation method for photooxidation of phenol. The layer silicate support had an extremely important effect on photocatalytic activity. As their interpretation, the recombination of photogenerated e^-/h^+ pairs following charge separation was inhibited by the force field of the clay support in contact with TiO_2 particles. Unfortunately, TiO_2 nanoparticles supported on montmorillonite often show low photocatalytic activity due to the amorphous phase and the poor accessibility to the TiO_2 surface [18]. Therefore, it is still a large challenge for design and fabrication of novel immobilized TiO_2 on montmorillonite with high photocatalytic activity.

In the present work, novel silica and titanium dioxide immobilized organoclay hybrids with high adsorption capability and high photocatalytic activity are synthesized via hydrothermal sol–gel method. The negatively charged silica particles act an important role in uniformly dispersing TiO_2 on organoclay layers and tailoring the particle size of TiO_2, which results in great enhancement of photocatalytic activity. The high adsorption capability of organoclay is favorable to enrich the organic compounds around the photoactive centers. Therefore, combination of adsorption and heterogeneous photocatalysis is an effective and cost-effective method for removal of organic compounds from wastewater.

2 Experimental

2.1 Materials

Na-montmorillonite (Na-MMT), with cation exchange capacity (CEC) of 90 meq/100 g of clay, was purchased from Zhangjiakou Qinghe Chemical Factory, China. Cetyltrimethylammonium bromide ($C_{16}H_{33}N^+(CH_3)_3Br^-$, CTAB), tetra-*n*-butyl titanate ($Ti(OC_4H_9)_4$, TBT) and tetraethylorthosilicate ($Si(OC_2H_5)_4$, TEOS) were purchased from Beijing Chemical Reagent Co. All the chemical agents were used as received without further purification.

2.2 Synthesis of SiO_2/TiO_2–organoclay hybrids

SiO_2/TiO_2–organoclay hybrids were synthesized via one-pot method. Na-montmorillonite was firstly organically modified to obtain organoclay (OMMT) by cation exchanging with CTAB in a three-neck flask at 353 K for 3 h. The mixture of silica and titania sol solution was added dropwise into the flask under continuously stirring. The silica sol solution was prepared by mixing TEOS, 2N HCl and ethanol in the volume ratio of 17.8/4/18 at room temperature. The titania sol solution was obtained by adding TBT into 2N HCl with vigorously stirring. The molar ratio of H^+/Ti was 5. In order to control hydrolysis rate, TBT was premixed with ethanol with the volume ratio of 1/2. After aging for 3 h at room temperature, the silica sol solution and the titania sol solution were mixed and stirred for further 30 min before adding into the organoclay suspension. After further stirring for 10 h at 353 K, the solid products were separated by filtering, followed by washing with a 1:1 (v:v) ethanol–water mixture, drying, and pulverizing. The powder samples were labeled as STOM0, STOM1 STOM2, and STOM4 with the ratio of Si/Ti = 0, 1, 2, 4, respectively. The ratio of Ti/clay was fixed at 5 mmolTi g^{-1} clay.

2.3 Characterization

Powder X-ray diffraction patterns were performed on a Rigaku D/max 2400 diffractometer using Cu Kα radiation ($\lambda = 0.154$ nm) at a generated voltage of 40 kV and current of 120 mA at room temperature, and the scanning rate is 2°/min. FT-Raman spectra were recorded on a Bruker RFS100/S FT-Raman spectrometer equipped with an InGaAs detector. JEOL S-4300F field emission scanning electron microscope (SEM) at 15 kV and JEOL JEM-2010 transmission electron microscope (TEM) at 200 kV was used to observe the morphology of the samples. Infrared spectra were acquired from KBr pellets with a Perkin-Elmer System 2000 FT-IR spectrophotometer in the wave-number range of 4,000–370 cm^{-1} with a spectra resolution of 4 cm^{-1}.

2.4 Photodegradation experiments

Methyl orange (MO) was selected as a model pollutant to evaluate the adsorption capability and photoactivity of SiO_2/TiO_2–organoclay hybrids since MO was an azo dye

that was poisonous and difficult to be degraded biologically. Twenty milligram of SiO_2/TiO_2–organoclay hybrids were added into 100 mL of MO solution with a concentration at 15 mg L^{-1}. Before UV irradiation, MO solutions containing the photocatalysts were magnetically stirred in dark for 3 h to achieve adsorption equilibrium. The equilibratory concentration after adsorption was fixed as the initial concentration (C_0) of the succeeding photodegradation. The photocatalytic degradation experiment was carried out under Xe lamp at room temperature. The light intensity was about 200 μW cm^{-2}, as measured by a UV radiometer. The change of MO concentration (C_t) was monitored by recording the absorbance at 464 nm with UV–Vis spectroscopy (Shimadzu UV1601-PC) at fixed intervals.

3 Results and discussion

Figure 1 shows the XRD patterns of SiO_2/TiO_2–organoclay hybrids. The interlayer spacing (d_{001}) increases from 0.96 nm up to 1.98 nm for OMMT, STOM0, STOM1 and STOM2, due to the intercalation of the cationic surfactant. However, for STOM4, the d_{001} is 1.44 nm. The decrease of interlayer spacing is probably ascribed to the formation of cross-linked structure between silica and clay at high silica amount [19]. The enlarged interlayer spacing can increase the adsorption capability for organic compounds within the space of silicate lamellae. Moreover, the nature of clay is changed from hydrophilic to hydrophobic after modification. The hydrophobic surface makes it easy for organic compounds to adsorb on clay layers. Furthermore, the peaks appearing at $2\theta = 25.3°$, 38.7°, 47.6°, and 54.8° are attributed to anatase phase. With increasing the ratio of Si/Ti, the intensity of the characteristic peak at $2\theta = 25.3°$ is gradually decreased, suggesting that the average particle size of TiO_2 is reduced. Table 1 lists the average particle sizes (D) calculated by Scherrer's equation. The average particle size of TiO_2 immobilized on organoclay is decreased from 14.9 nm down to 7.0 nm by introduction of the negatively charged silica. This may be due to that the silica matrix prevents diffusion or coalescence of TiO_2 nanoparticles during ripening process. The reduced particle size is favorable to improve the photodegradation efficiency since the photoactivity is influenced by surface area, crystalline phase, and particle size. In addition, immobilization of SiO_2 and TiO_2 on organoclay has little effects on the interlayer spacing, suggesting that the particles is mainly distributed on the surface of organoclay layers but not within the interlayer space.

Table 1 Structure parameters of SiO_2/TiO_2–organoclay hybrids

Sample	Ti mmol/g clay	Molar ratio of Si/Ti	d_{001} (nm)	D (nm)
STOM0	5	0	1.91	14.9
STOM1	5	1	1.85	8.4
STOM2	5	2	1.85	7.2
STOM4	5	4	1.44	7.0

XRD patterns usually reveal long-range order of materials and provide average structural information within several unit cells, while Raman spectroscopy is sensitive to local crystalline domains. Figure 2 shows the Raman spectra of SiO_2/TiO_2–organoclay hybrids with different Si/Ti ratios. Four well-resolved peaks at 157, 415, 505, and 626 cm^{-1} presented in the Raman spectra are the characteristic peaks of anatase TiO_2 [20]. The peak intensity at 157 cm^{-1} exhibits a gradual decrease with increasing the

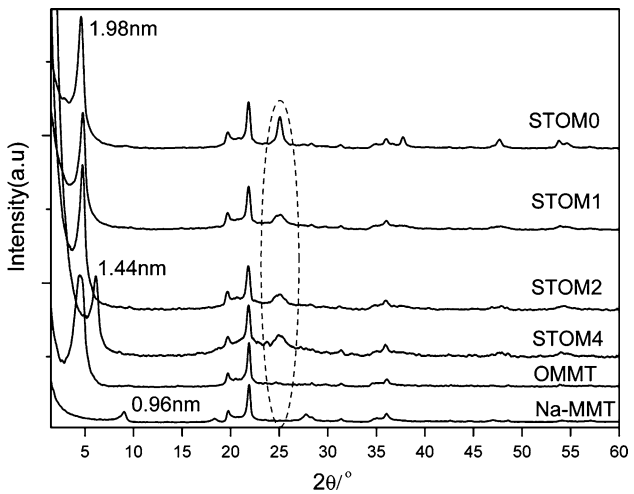

Fig. 1 XRD patterns: (**a**) STOM0, (**b**) STOM1, (**c**) STOM2, (**d**) STOM4, (**e**) OMMT, and (**f**) Na-MMT

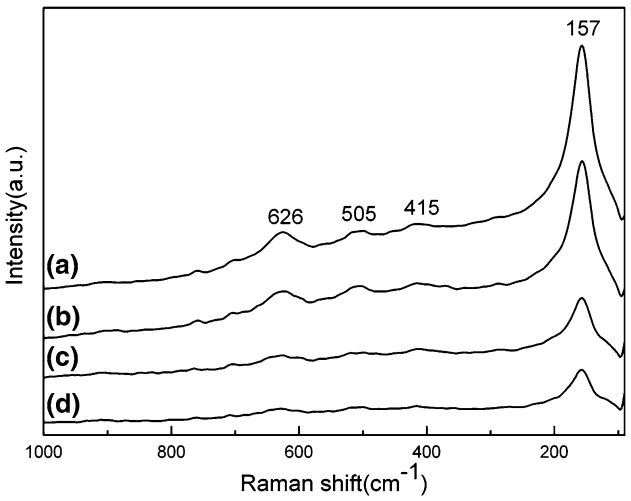

Fig. 2 Raman spectra of: (**a**) STOM0 (**b**) STOM1, (**c**) STOM2, and (**d**) STOM4

ratio of Si/Ti. In Raman spectrum, the intensity and full-highest maximum width at the low-frequency peak is closely related to the crystallite size and the crystalinity. When the crystallite dimension is reduced to the nanometer scale, the local lattice imperfections can cause Raman scattering effect, which results in the decrease of the intensity and broadening [20]. These results are well in agreement with XRD results, which further indicate that silica acts as a size-tailor.

In order to investigate the detail in structure, the morphologies of SiO_2/TiO_2–organoclay hybrids are directly observed on scanning electron microscope (SEM) and transmission electron microscopy (TEM). Figure 3a and b shows the SEM images of STOM0 and STOM2, respectively. It is obvious to see the difference in dispersion of inorganic nanoparticles on organoclay. In the case of STOM0 (only TiO_2 immobilized organoclay), TiO_2 nanoparticles are mainly distributed along the edges of organoclay layers. However, in STOM2, the nanoparticles are uniformly dispersed on entire organoclay layers. The differences of morphology are clearer observed in TEM images. As shown in Fig. 3c and d, shuttle-like TiO_2 nanoparticles with particle sizes of about 20 nm are formed along the edges of organoclay in STOM0, while homogeneous dispersion of TiO_2 nanoparticles with smaller size is found in STOM2.

A possible interpretation of the differences in dispersion of TiO_2 nanoparticles on organoclay layers is the electrostatic effect [21]. As for STOM0, the surfaces of clay layers are coated by cationic surfactants (CTAB), which hinders the proximity of the positively charged TiO_2 particles. However, at the edges of organoclay, TiO_2 sol particles can easily interact with the hydroxyl groups of clay layers by hydrogen bonds to form nucleation sites [22]. These nucleation sites lead to further growth of TiO_2 crystallites along the edges of organoclay. In contrast, the dispersion mechanism of TiO_2 nanoparticles is quite different for SiO_2/TiO_2–organoclay hybrids. On the one hand, the negatively charged silica sol particles reduce the repulsion between the cationic surfactants on organoclay and the positively charged titania sol particles. On the other hand, the addition of negatively charged silica sol particles increases the surface charge density. As we known, the surface energy, γA (γ is the interfacial tension and A is the

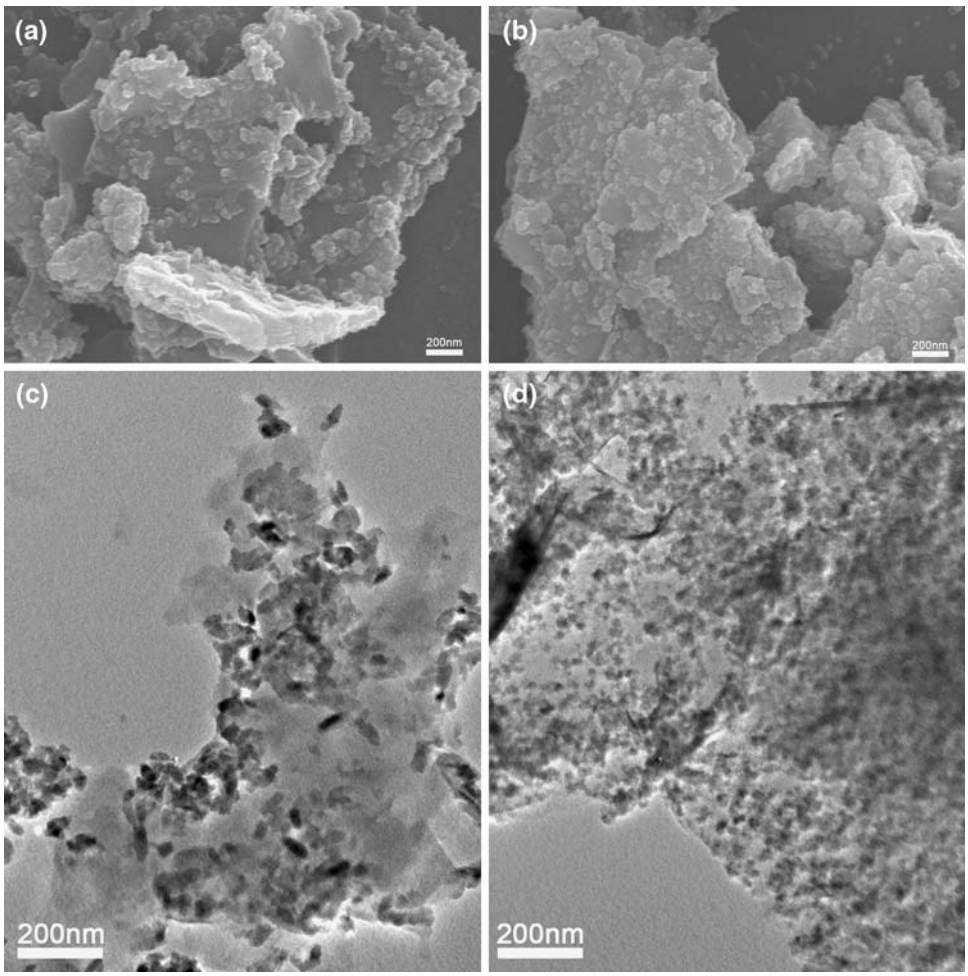

Fig. 3 SEM images for: (**a**) STOM0, (**b**) STOM2; TEM images for: (**c**) STOM0, (**d**) STOM2

surface area), is an important factor for the particle size. The interfacial tension is the driving force to decrease the surface area and form aggregation. As stated by Gibbs's law, $d\gamma = -\sum \Gamma_i \mu_i$, with Γ_i the density of adsorption of species i of electrochemical potential μ_i, the interfacial tension can be lowered by adsorption or by the electrostatic charge effect [23]. As the negatively charged silica is introduced into the system, the increased surface charge density can reduce the interfacial tension. Consequently, TiO_2 nanoparticles can achieve uniform dispersion on organoclay layers during the immobilization process.

To further understand the effect of silica on the dispersion of TiO_2 nanoparticles on organoclay, FT-IR spectra are measured for OMMT, STOM0, STOM2, and calcined STOM2 at 800 °C for 2 h (Fig. 4). The peak corresponding to the vibration of Si–O–Ti bond at ca. 946 cm^{-1} are absent in the spectra of OMMT, STOM0 and STOM2, except for calcined STOM2. It suggests that no chemical reaction between TiO_2 and SiO_2 occurs at low temperature (80 °C in our case). This result provides strong evidence that TiO_2 nanoparticles are independently dispersed on the surface of organoclay without forming any distinct chemical bonding with silica in the hybrids. TiO_2 nanoparticles separated by silica matrix avoid the formation of aggregation. The smaller TiO_2 nanoparticles with high surface area and uniform dispersion can increase the number of photoactive centers, and enhance the photocatalytic activity effectively.

Organic dyes from industry are the refractory pollutants in wastewater. In this work, methyl orange (MO) is selected as a model pollutant to evaluate the adsorption capability and photocatalytic activity of SiO_2/TiO_2–organoclay hybrids. In the removal of MO from water, there are two factors resulting in the decrease of MO concentration: the adsorption of MO on the photocatalysts and the photocatalytic degradation under UV irradiation. Table 2 lists the changes of MO concentration during the removal process. Compared with the initial MO concentrations (C_0), the concentrations after adsorption (C_A) are decreased drastically, particularly in the case of STOM0. Here, the removal efficiency (E) is use to describe the decolorizing process, expressed as $E = (C_0 - C)/C_0$. All the samples show high adsorption efficiencies (E_A), greater than 75%. With increasing the silica content, the adsorption efficiency is decreased. This may be due to the coating effect of silica matrix on organoclay, which limits the adsorption of MO. High adsorption capability can ensure that high pollutant concentration regions are formed around the photoactive centers, where the pollutants can easily contact with the photocatalysts. As irritated in UV light, the concentrations of MO after photodegradation process (C_P) are further decreased. Combining the adsorption and photodegradation, the total removal efficiency (E_T) is higher than 85%. Figure 5 shows the changes of MO concentration with UV irradiation time during photodegradation process. The concentration after adsorption, C_A, is fixed as the initial concentration of the photodegradation process. It reveals that SiO_2/TiO_2–organoclay hybrids have higher photocatalytic activity than that of only TiO_2 nanoparticles

Table 2 Changes of MO concentration during adsorption and photodegradation process

Sample	C_0 (mg/L)	C_A (mg/L)	E_A (%)	C_P (mg/L)	E_T (%)
STOM0	15	0.93	93.8	0.81	94.6
STOM1	15	2.50	83.3	1.08	92.8
STOM2	15	3.48	76.8	0.41	97.3
STOM4	15	3.37	77.5	2.22	85.2

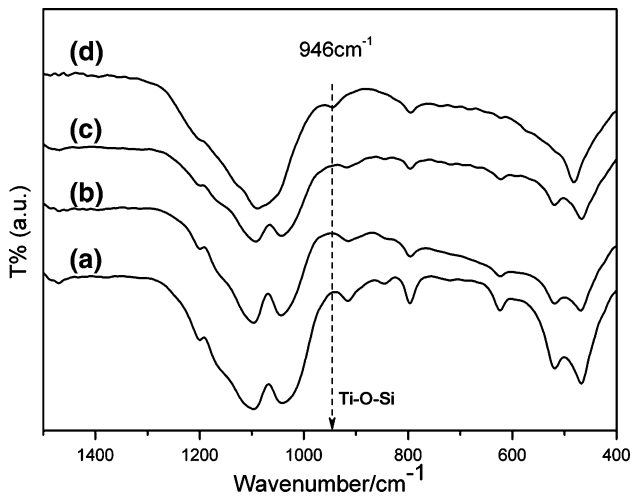

Fig. 4 FT-IR transmittance spectra for (**a**) OMMT, (**b**) STOM0, (**c**) STOM2, and (**d**) calcined STOM2

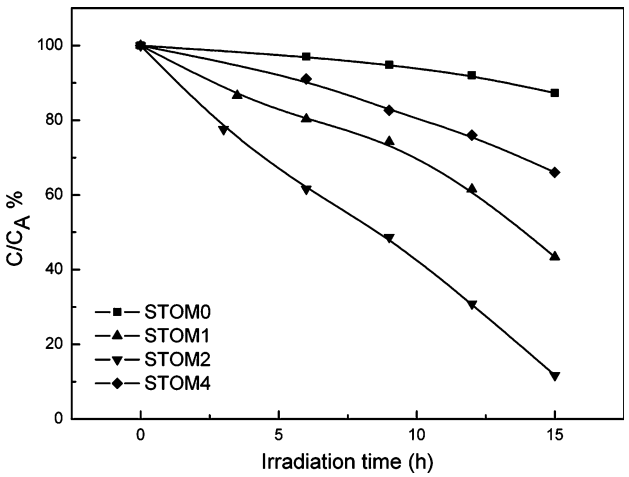

Fig. 5 Variations of MO concentration under photocatalytic degradation

immobilized organoclay. Although STOM0 shows a higher adsorption capability, the concentration of MO after photodegradation (C_P) was decreased slightly because of its low photocatalytic. The low photocatalytic activity limits its application because the adsorbed organic compounds may cause secondary pollution of environment unless they are decomposed completely. Furthermore, the addition of silica has an optimum amount for the photoactivity. At higher silica content, the nanoscaled TiO_2 surrounded by silica matrix is hindered to interact with organic compounds, and thereby decreases the photocatalytic efficiency. In summary, the higher photoactivity of SiO_2/TiO_2–organoclay hybrids may be attributed to three factors. Firstly, silica acts as a size-tailor and reduced the particle size of TiO_2. The smaller size of TiO_2 can increase the photoactivity greatly. Secondly, the uniform dispersion of TiO_2 on organoclay layers increases the numbers of the photoactive sites. Thirdly, the high adsorption capability of organoclay enriches the pollutants on the surface of photocatalysts. The proximity of the adsorption site to the photoactive sites in this structure improves the diffusion of the adsorbed pollutants to photoactive sites. Once the pollutants interact with oxide species photogenerated on the surface of TiO_2, they will be photodegraded and mineralized into CO_2 and H_2O. Moreover, SiO_2/TiO_2–organoclay hybrids can be easily separated from the suspension after photodegradation in several minutes when the stirring is stopped. The small particles in the hybrids are immobilized on organoclay layers to form large granules which can be easily recovered from the purified water by filtration or sedimentation. Therefore, SiO_2/TiO_2–organoclay hybrids are promising photocatalysts in practical application.

4 Conclusion

In this work, novel SiO_2/TiO_2–organoclay hybrids with high adsorption capability and high photocatalytic activity were synthesized by immobilizing mixed silica and titania sol particles on organically modified clay. The addition of negatively charged silica played an important role in reducing TiO_2 particle size and dispersing nanosized TiO_2 on organoclay. On the one hand, negatively charged silica reduced interfacial tension by increasing the surface charge density. On the other hand, addition of negatively charged silica reduced the repulsion between cationic surfactants and positively charged titania sol particles, which facilitated the homogeneous dispersion of TiO_2 nanoparticles on entire clay layers. The high adsorption capability is favorable for pollutants diffusing to the photocatalytic sites on SiO_2/TiO_2–organoclay hybrids. The combination of adsorption of organoclay and heterogeneous photocatalysis of TiO_2 nanoparticles is a promising technique in removal of organic pollutants in wastewater.

Acknowledgements This work was financially supported by the National Natural Science Foundation of China (Grant nos. 50473054 and 50533070) and the Major Basic Research Projects of China (Grant 003CB615600).

References

1. Theng BKG (1974) The chemistry of clay-organic reactions. Wiley, New York
2. Ogawa M, Kuroda K (1997) Bull Chem Soc Jpn 70:2593
3. Shen YH (2002) Water Res 36:1107
4. Boyd SA, Lee J-F, Mortland MM (1988) Nature 333:345
5. Jaynes WF, Boyd SA (1991) Soil Sci Soc Am J 55:43
6. Wagner J, Chen H, Brownawell BJ, Westall JC (1994) Environ Sci Technol 28:231
7. Celik A, Yildiz N, Calimli A (1999) Rev Chem Eng 15:349
8. Dentel SK, Bottero JY, Khatib K, Demougeot H, Duguet JP, Anselme C (1995) Water Res 29:1273
9. Koh SM, Dixon JB (2001) Appl Clay Sci 18:111
10. Hoffmann MR, Martin ST, Choi WY, Bahnemann DW (1995) Chem Rev 95:69
11. Fujishima A, Hashimoto K, Watanabe T (1999) TiO_2 photocatalysis: fundamentals and applications. BKC Inc., Tokyo
12. Wan-Kuen J, Park KH (2004) Chemosphere 57:555
13. Nagaveni K, Sivalingam G, Hegde MS, Madras G (2004) Environ Sci Technol 38:1600
14. Ao CH, Lee SC, Yu JC (2003) J Photochem Photobiol A-Chem 156:171
15. Xu YM, Langford CH (1997) J Phys Chem B 101:3115
16. Bhattacharyya A, Kawi S, Ray MB (2004) Catal Today 98:431
17. Kun R, Mogyorosi K, Dekany I (2006) Appl Clay Sci 32:99
18. Zhu HY, Li JY, Zhao JC, Churchman GJ (2005) Appl Clay Sci 28:79
19. Letaief S, Martin-Luengo MA, Aranda P, Ruiz-Hitzky E (2006) Adv Funct Mater 16:401
20. Zhang WF, He YL, Zhang MS, Yin Z, Chen Q (2000) J Phys D Appl Phys 33:912
21. Pottier AS, Cassaignon S, Chaneac C, Villain F, Tronc E, Jolivet JP (2003) J Mater Chem 13:877
22. Tyagi B, Chudasama CD, Jasra RV (2006) Appl Clay Sci 31:16
23. Stol RJ, DeBruyn PL (1980) J Colloid Interf Sci 75:185